



Photo-degradation of atmospheric chromophores: type conversion and changes in photochemical reactivity

Zhen Mu^a, Qingcai Chen^{a*}, Lixin Zhang^a, Dongjie Guan^a and Hao Li^a

^a *School of Environmental Science and Engineering, Shaanxi University of Science and Technology, Xi'an 710021, China*

*Corresponding authors:

School of Environmental Science and Engineering, Shaanxi University of Science and Technology, Weiyang District, Xi'an, Shaanxi, 710021, China.

*(Q. C.) Phone: (+86) 0029-86132765; e-mail: chenqingcai@sust.edu.cn;



1 **Abstract:** Atmospheric chromophoric organic matters (COM) can participate in photochemical
2 reactions because of the photosensitiveness, thus COM have a potential contribution to aerosols
3 aging. The photochemical mechanism of atmospheric COM and the effect of photo-degradation on
4 its photochemical reactivity are not fully understood. To address this knowledge gap, the
5 characteristics of COM photo-degradation and the potential effects of COM photolysis on the
6 photochemical reactivity are illustrated. COM are identified by excitation-emission matrices
7 combined with parallel factor analysis. We confirm that both water-soluble and water-insoluble
8 COM are photo-bleached, and an average 70% of fluorescence intensities are lost after 7 days of
9 light exposure. Furtherly, it is found that there is a transformation process of low oxidation to high
10 oxidation HULIS. We propose that the high oxidation HULIS could be used to trace the aging
11 degree of aerosols. In terms of photochemical reactivity, compared with before photolysis, the triplet
12 state COM ($^3\text{COM}^*$) decrease slightly in ambient particle matter (ambient PM) samples and
13 increase in primary organic aerosol (POA). However, the COM induce fewer singlet oxygen after
14 photolysis. The photolysis and conversion of COM are the major cause of the change of
15 photochemical activity. The result also enunciate that the photochemical reaction mechanisms and
16 aerosol aging processes are relatively different in various aerosols. In conclusion, we demonstrated
17 that the photo-degradation of COM not only change the chemical compositions, but also change the
18 roles of the COM in the aerosol aging process.

19 **Key word:** atmospheric chromophores; photo-degradation; EEMs; triplet state; reactive oxygen
20 species.

21



22 1. Introduction

23 Chromophoric organic matters (COM) widely exist in the atmospheric environment. COM are
24 mainly derived from biomass combustion emissions and secondary chemistry reactions (Andreae
25 and Gelencser, 2006; Graber and Rudich, 2005; Zappoli et al., 1999). Because of the significant
26 absorption for short wave radiation (the range of near-ultraviolet light to visible light) (Rosario-
27 Ortiz and Canonica, 2016; Cheng et al., 2016), COM may have a significant effect on the
28 atmospheric composition through photolysis, photo-conversion and inducing reactive substances
29 (Chen et al., 2018; Wenk et al., 2011; Maizel et al., 2017). Simulation and evaluation of COM
30 photochemistry improve understanding the mechanism of the aerosol aging.

31 As photosensitive substances in aerosol, the physical and chemical characteristics of COM
32 change significantly under sunlight exposure (Kieber et al., 2012; Lee et al., 2013; McKnight et al.,
33 2001; Murphy et al., 2013; Cory and McKnight, 2005; Korak et al., 2014; Chin et al., 1994). The
34 specific impacts are summarized. (1) Changes in optical characteristics. Sunlight exposure can cause
35 the photo-bleaching of COM. Previous studies shown that chromophores produced by wood-
36 burning were significantly photo-bleached in aerosols (Lee et al., 2014; Zhong and Jang, 2014). Yet
37 the mechanisms of photo-bleaching process are still not complete clear. (2) Changes in chemical
38 composition. Photochemistry have a significant effect on the composition of COM, because
39 photolysis cause that COM decompose into small molecules. Therefore, COM may have lower
40 volatility and higher oxidation degree after photolysis (Vodacek et al., 1997; Del Vecchio and
41 Blough, 2002; Gonsior et al., 2009; Grieshop et al., 2009). In contrast, COM could also be generated
42 due to photochemical reaction. For example, oligomeric COM could be generated by a mixture of
43 anthracene and naphthalene suspensions due to self-oxidation under light conditions; photo-
44 oxidation of aromatic isoprene oxides are an important source of high-molecular-weight COM
45 (Altieri et al., 2006; Altieri et al., 2008; Haynes et al., 2019; Holmes and Petrucci, 2006; Perri et al.,
46 2009). Changes in chemical composition affect photochemical activity in turn. Therefore, it is
47 crucial to illustrate the changes in optical characteristics and chemical composition, which could
48 promote understanding the characteristic and mechanisms of COM photochemistry in aerosols.

49 Atmospheric COM not only decompose and transform, but also participate in the complex
50 photochemical reaction, which further affect the aerosol aging (Malley et al., 2017). On the one
51 hand, COM could participate in atmospheric photochemical processes directly. For example,
52 excited COM react with organic matters and promote secondary organic aerosols (Zhao et al., 2015;
53 Saleh et al., 2013; Zhong and Jang, 2014; Lee et al., 2014; Liu et al., 2016). Various secondary
54 photochemical processes also increase the complexity of COM composition (Wenk et al., 2011;
55 Zhou et al., 2019; Smith et al., 2014; Richards-Henderson et al., 2015; Kaur and Anastasio, 2018;
56 Chen et al., 2016a and b). On the other hand, COM also participate in atmospheric photochemical
57 reactions indirectly because COM can induce reactive species. Powers et al. (2015) probed the
58 photochemical activity of the deep ocean refractory dissolved organic carbon (DOC) through
59 simultaneous measuring the rates of both H_2O_2 and O_2^- photoproduction in the laboratory.



60 Photochemical activity is universal feature of DOC. For example, aromatic ketones could be excited
61 to generate triplet state ($^3\text{COM}^*$) under light conditions (Rosario-Ortiz and Canonica, 2016; Del
62 Vecchio and Blough, 2004; Wenk et al., 2013; Ma et al., 2010). $^3\text{COM}^*$ induce reactive oxygen
63 species (ROS), such as singlet oxygen ($^1\text{O}_2$), super-oxygen ($\bullet\text{O}_2^-$) and hydroxyl ($\bullet\text{OH}$), which could
64 drive aerosol aging (Paul Hansard et al., 2010; Szymczak and Waite, 1988; Zhang et al., 2014;
65 Rosario-Ortiz and Canonica, 2016; Sharpless, 2012; Haag and Gassman, 1984). COM have the
66 potential effects on aerosol aging, so it is necessary to clarify the path of COM driving aerosol aging.

67 In order to illustrate the effect of COM photo-degradation on the optical properties and
68 photochemical reactivity in aerosols, we simulate the photolysis process of primary organic aerosol
69 (POA) and ambient particle matter (ambient PM) in laboratory. The characteristics of photo-
70 degradation in water-soluble and water-insoluble chromophores are clarified by the approach of
71 excitation-emission matrices (EEM) combined with parallel factor analysis (PARAFAC). The
72 effects of aerosol aging on photochemical reactivity (photochemical reactivity is characterized by
73 triplet state and singlet oxygen generation capacity) are also stated by reactive species capture
74 technology and electron paramagnetic resonance spectrometer (EPR).

75 2. Experimental Section

76 2.1 Sample Collection

77 A total of 16 samples were collected (The details of the samples are shown in Table S1 of SI).
78 The ambient PM samples were collected in Shaanxi University of Science and Technology, Xi'an,
79 Shaanxi Province (N34°22'35.07", E108°58'34.58"; the sampling device is about 30 m from the
80 ground). The ambient PM samples were collected on a quartz fiber filter (Pall life sciences, Pall
81 Corporation, America) by an intelligent large-flow sampler (Xintuo XT-1025, Shanghai, China)
82 with a sampling time of 23 h 30 min and a sampling flow rate of 1000 L/min. The ambient PM
83 samples were stored in the refrigerator at -20 °C prior to use.

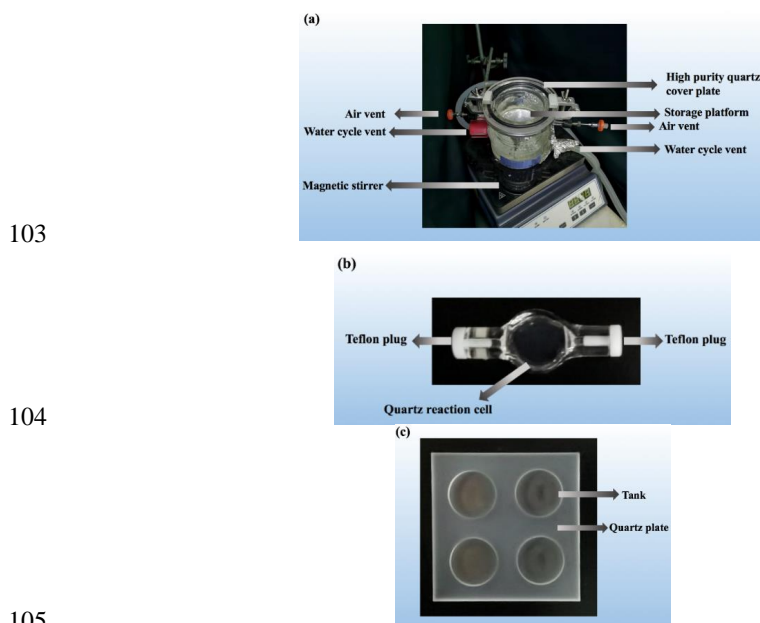
84 The POA samples were collected through a combustion chamber. Wheat straw, corn straw,
85 rice straw and wood were burned at about 500 °C in the tube stove. The clean air was introduced at
86 a flow rate of 2 L/min to ensure complete combustion. The particle matters entered the collected
87 chamber. The clean air was introduced into the collected chamber at a flow rate of 2 m³/h to dilute
88 the combustion gas. POA samples were collected on the quartz fiber filter (Pall life sciences, Pall
89 Corporation, America) with a diameter of 37 mm. The POA sample were stored in the refrigerator
90 at -20 °C prior to use.

91 2.2 Photolysis experiment

92 A high-purity quartz reactor was designed for the photolysis experiment (**Fig.1a**). A rubber
93 gasket was embedded on the upper edge of the reactor. The reactor was clamped with a high-purity
94 quartz cover to form a sealed environment. Two vents were designed in the low position of the
95 reactor. The vents were connected to water circulator to ensure that the temperature was about 25°C
96 in the reactor. The reactor was placed on a magnetic stirrer and the rotation speed was 200 rpm to
97 stabilize the temperature and humidity (~50%). A xenon lamp was equipped with a VISREF light



98 filter (PLS-SXE 300, Perfectlight, China) to simulate sunlight (The wavelength spectrum of the
99 xenon lamp is shown in Figure S1 of SI). The light intensity per unit area was about 1.2-1.3 times
100 the solar light at 12:00, at N34°22'35.07", E108°58'34.58". A support was placed in the reactor and
101 the samples were placed on the support. The illumination time were 0 h, 2 h, 6 h, 12 h, 24 h, 3 d and
102 7 d, respectively.



103

104

105

106 **Fig.1** Schematic diagrams of the photochemical devices. (a) The reactor is used for maintaining the reaction
107 environment. The water cycle vents are connected with a water circulator to maintain the temperature. (b) The reactor
108 is used for triplet state experiments. The reactor is made of quartz. The plugs are made of Teflon. The internal
109 volume is 200 μL . (c) A reactor is used for the experiment of triplet state inducing singlet oxygen. The size of quartz
110 plate is $35 \times 35 \text{ mm}^2$. The size of the tanks is a radius of 5.6 mm and a depth of 2.5 mm.

111 2.3 Sample extraction

112 The samples extracts were obtained by the approach of ultrasonic extraction. The original and
113 photolyzed samples were extracted with ultra-pure water ($>18.2 \text{ M}\Omega \cdot \text{cm}$, Master series, Hitech,
114 China) and the suspensions were filtered through a $0.45 \mu\text{m}$ filter (Jinteng, China) to obtain the
115 water-soluble organic matter (WSOM). After water extraction, the samples were further extracted
116 with methanol (HPLC Grade, Fisher Chemical, America) to obtain water-insoluble organic matter
117 (WISOM) using the above method. The blank samples were also extracted. The specific extraction
118 method was the same as sample extraction, which was used to correct the effect of the background.

119 2.4 OC/EC analysis

120 The method of organic carbon (OC) analysis could refer to the previous literature (Mu et al.,
121 2019). Briefly, 100 μL of extracts were injected on the clean quartz filter. Then, the filters were
122 dried out with a rotary evaporator. Carbonaceous components were analyzed by the OC/EC online



123 analyzer (Model 4, Sunset, America) with the approach of NIOSH 870 protocol (Karanasiou et al.,
124 2015). Six parallel samples were analyzed and the results showed that the uncertainty of the method
125 was <3.7% (one standard deviation).

126 2.5 Optical analysis

127 The light absorption and EEM spectra of the extracts were analyzed by an Aqualog
128 fluorescence spectrophotometer (Horiba Scientific, America). The extracts were diluted for optical
129 analysis (The concentrations are shown in Table S2 of SI). The absorption spectra were recorded in
130 the wavelength range of 200-600 nm. The range of excitation wavelength was 200-600 nm and the
131 range of excitation wavelength was 250-800 nm. The interval was 5 nm. The exposure time was 0.5
132 s. The background samples were also analyzed using the same method and the background signals
133 were subtracted from the sample signals.

134 The EEM data was analyzed by the PARAFAC model to identify chromophores (The detailed
135 analysis process refer to the previous papers) (Chen et al., 2016b; Chen et al., 2016a). Briefly,
136 according to the EEM characteristics and the residual error variation trend of the 2-7 component
137 PARAFAC models, 4 component PARAFAC model was selected (Analysis error of the models are
138 shown in Figure S2 of SI).

139 2.6 Triplet state generation experiment

140 The triplet states generation ability before and after photolysis were studied. Chemical probe
141 2,4,6-trimethylphenol (TMP) was used as the capturing agent for the triplet state. 60 μL of WSOM
142 extracts (OC concentrations are shown in Table S3) and 60 μL of TMP solution ($c_{\text{TMP}} = 20 \mu\text{M}$,
143 Aladdin, China) were mixed in the cell (**Fig.1b**). The cell was placed in the reactor (**Fig.1a**) and the
144 reaction conditions were the same as shown in 2.2. The illumination time was 0, 5, 10, 15, 30, 45,
145 60 and 90 min, respectively. 90 μL mixed solution was taken out from the cell at different time
146 points. Then 30 μL of phenol solution ($c_{\text{phenol}} = 50 \mu\text{M}$, Aladdin, China) were added into the mixed
147 solution (Phenol solution was used as the internal standard substance for TMP quantification). TMP
148 was quantified by liquid chromatography (LC).

149 The analyzed parameters of LC are as follows: C18 column (Xuanmei, China); mobile phase:
150 acetonitrile/water = 1/1 (v/v); flow rate: 1 mL/min; UV detector: detection wavelength 210 nm.
151 Kaur and Anastasio (2018) and Richards-Henderson et al. (2015) have found that TMP consumption
152 conform to first-order kinetics in the triplet state capture reaction. The first-order kinetic equation
153 was used to fit exponential relationship among the TMP concentration ($c_{\text{TMP}}/\mu\text{M}$), the illumination
154 time (t/min) and triplet state generation rate constants ($k_{\text{TMP}}/\text{min}^{-1}$):

$$155 \quad c_{\text{TMP}} = a \cdot e^{k_{\text{TMP}} \times t} \quad (1)$$

156 2.7 Triplet state driving singlet oxygen experiment

157 The effects of the photolysis on singlet oxygen in aerosols were studied. 4-Hydroxy-2, 2, 6, 6-
158 tetramethylpiperidine (TEMP, $c_{\text{TEMP}}=240 \text{ mM}$, Aladdin, China) was used as the capturing agent of
159 singlet oxygen and captured singlet oxygen was quantified by EPR spectrometer (MS5000, Freiberg,
160 Germany). Sorbic acid (SA, $c_{\text{SA}}=133.3 \mu\text{M}$, Aladdin, China) was used as quenching agent for triplet



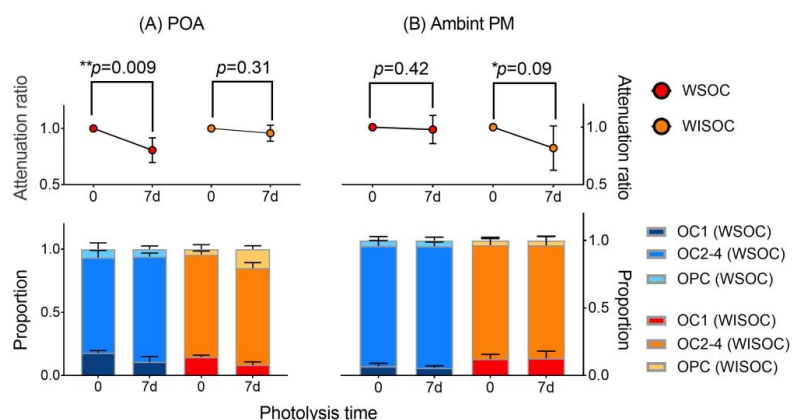
161 state. The method was as follows: (1) 40 μL WSOM, 40 μL TEMP and 40 μL ultra-pure water were
162 mixed in the tanks (**Fig.1c**). The mixed solution was placed in the reactor (**Fig.1a**). Then, 50 μL of
163 the mixed solution was taken out by capillary for EPR analysis; (2) 40 μL of WSOM, 40 μL of
164 TEMP and 40 μL of ultra-pure water were mixed. The mixed solution was placed in the reactor for
165 60 min without illumination. Then 50 μL of the mixed solution was taken out by capillary for EPR
166 analysis; (3) 40 μL of WSOM, 40 μL of TEMP and 40 μL of ultra-pure water were mixed in the
167 cell. The mixed solution was placed in the reactor for 60 min with illumination. 50 μL of the mixed
168 solution was taken out by capillary for EPR analysis; (4) 40 μL of WSOM, 40 μL of TEMP and 40
169 μL of SA solution were mixed in the cell. The mixed solution was placed in the reactor for 60 min
170 with illumination, then 50 μL of the mixed solution was taken out by capillary for EPR analysis.

171 **3. Results and discussion**

172 *3.1 Effect of COM photo-degradation on carbonaceous components*

173 Organic matters can be decomposed and transformed in aerosol due to illumination (Wong et
174 al., 2015). **Fig.2** describe the variable characteristics of total organic carbon and carbonaceous
175 components before and after COM photolysis. The results show that both water-soluble and water-
176 insoluble organic matter partially photolysis in POA samples (**Fig.2A**), with an average decrease of
177 22.1% and 3.5%, respectively. Compared with POA, WISOC decompose obviously in ambient PM,
178 with an average decrease of 26.3%, while the WSOC do not change significantly (**Fig.2B**).

179 Photolysis also result in the variation on carbonaceous components. In POA samples (**Fig.2A**),
180 the relative content of the OC1 (OC1 and OC2-4 are the different stage in the process of thermal-
181 optical analysis) decrease, which is the main loss of OC. The organic matters in the OC1 stage are
182 characterized by small molecular weight and highly volatile (Karanasiou et al., 2015). The result
183 shows that OC1 has a stronger ability of photo-decompose. On the other hand, the pyrolysis carbon
184 (OPC) in WISOM show an increasing trend (an average increase of 2.4 times). Generally, the
185 pyrolysis carbon is oxygen-containing substance. Thus, the increase of oxygen-containing organics
186 may be due to the aerosols aging. Contrast with POA, the carbonaceous components are relatively
187 stable in ambient PM (**Fig.2B**). The result reflect that ambient PM samples have been subjected to
188 sufficient atmospheric oxidation, so organic matters are not decomposed or oxidized again.

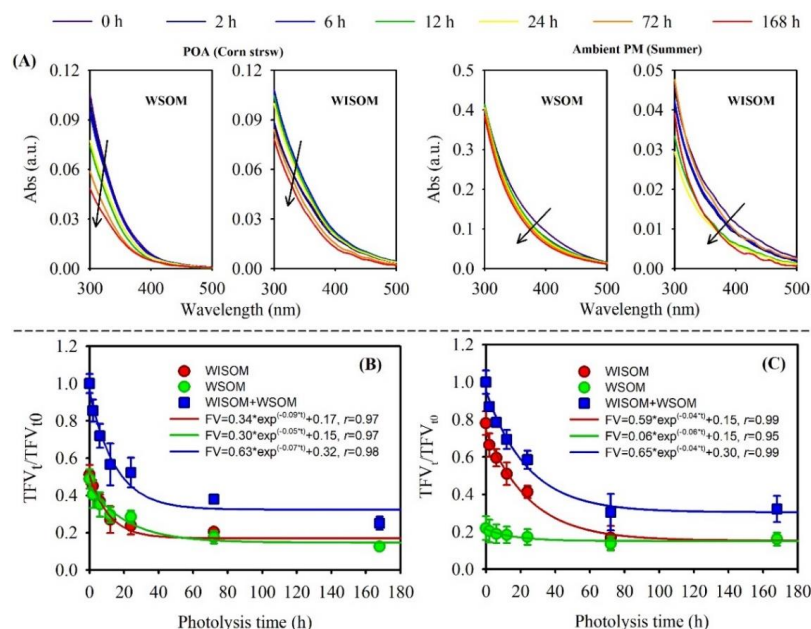


189

190 **Fig.2** Variations of total carbon and carbonaceous components before and after photolysis. The p -value is the
191 probability that two sets of data have the same level (two-tailed test). * and ** are represent the significant difference
192 at the 0.1 and 0.01 levels, respectively.

193 3.2 Effect of COM photo-degradation on optical properties

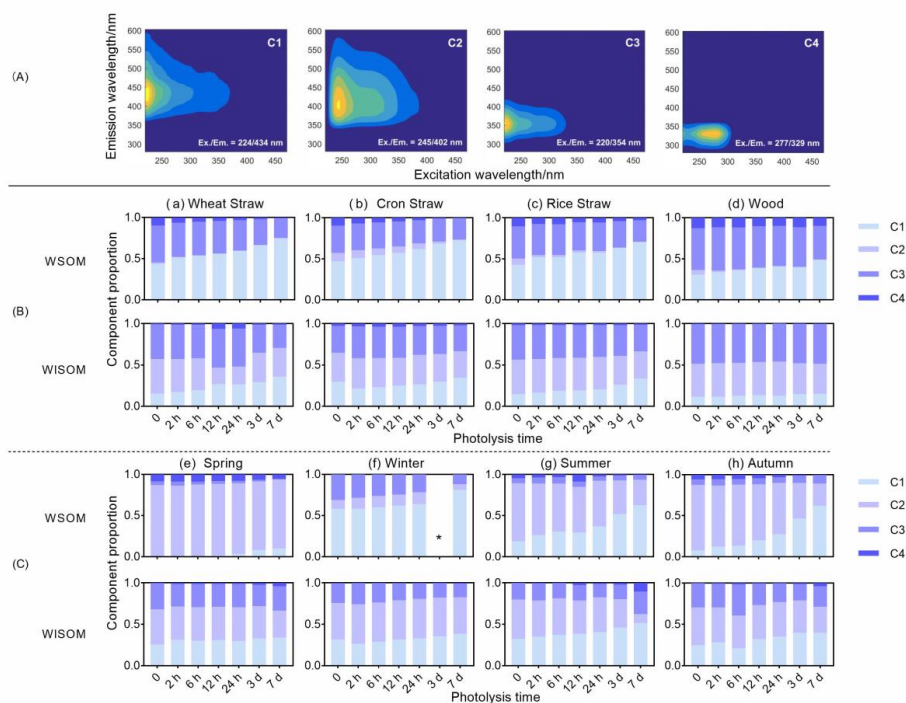
194 Both absorbance and total fluorescence volume (TFV, $\text{RU}\cdot\text{nm}^2/\text{m}^3$) represent an obvious
195 decreasing trend due to aerosol photolysis (**Fig.3**). Changes in optical properties are shown in Figure
196 S3, S4 and S5. The decrease of absorbance confirm that COM are photo-bleached (Duarte et al.,
197 2005). The subduction function of photolysis on absorbance is significant (Aiona et al., 2018). In
198 POA (**Fig.3B**), TFV decrease by 74.8% on average and the attenuation characteristics of water-
199 soluble and water-insoluble components are similar. The attenuation of fluorescence intensities is
200 different from Aiona's paper (Aiona et al., 2018). Changes in fluorescence intensities may depend
201 on the types of COM and the photochemical environment. Exceptionally, the water-insoluble
202 component of wood burning only decrease by 9.0% (Figure S5), which is significantly different
203 from other POA samples. The characteristics of TFV and WISOC of wood burning (section 3.1) are
204 similar, which probably attribute to the slight generation of secondary water-insoluble organic
205 substances. The characteristics of TFV attenuation in ambient PM (rate constant $k = 0.04 \text{ h}^{-1}$) is
206 different from POA ($k = 0.07 \text{ h}^{-1}$). Compared with water-soluble chromophores, the water-insoluble
207 chromophores photo-decompose obviously and the TFV decrease by 79.1%. In contrast, changes in
208 the water-soluble chromophores are only 21.9% on average, while 48.8% in POA samples. The low
209 attenuation result from COM have undergone a long-term atmospheric aging process and the water-
210 soluble COM are easier to photolysis.



211
 212 **Fig.3** The changes of light absorption and fluorescence volume in the photolysis process. (A) The light absorption
 213 spectrum. (B) and (C) show the attenuation curve of average fluorescence volume of POA (except for the wood
 214 sample) and ambient PM samples, respectively.

215 Four types of COM are identified by the approach of EEMs-PARAFAC and the composition
 216 variations are studied (**Fig.4A**). The fluorescence peaks of C1 and C2 appear at (Ex./Em. = 224/434
 217 nm) and (Ex./Em. = 245/402 nm), and the characteristics are similar to high and low oxidation
 218 HULIS, respectively (Chen et al., 2016b; Birdwell and Engel, 2010). The peaks of C3 and C4 appear
 219 at (Ex./Em. = 220/354 nm) and (Ex./Em. = 277/329 nm) and these two chromophores were
 220 identified as protein-like organic matters (PLOM-1 and PLOM-2) in previous studies (Sierra et al.,
 221 2005; Huguet et al., 2009; Chen et al., 2016a and 2016b; Coble, 2007; Fellman et al., 2009).

222 The compositions of chromophores change significantly in the photolysis process. In POA
 223 (**Fig.4B**), the high-oxidation HULIS show an obvious increasing trend in water-soluble component
 224 and the relative content increase by 25.7% on average. On the contrary, low oxidation HULIS and
 225 PLOM show a decreasing trend and the relative attenuation are 6.0% and 19.7%, respectively. The
 226 proportion variation indicate that high-oxidation HULIS chromophores could be generated in the
 227 photochemistry process and low oxidation HULIS and PLOM chromophores may be photolyzed
 228 (Tang et al., 2020; Chen et al., 2020). Not only in water-soluble chromophores, the content of high-
 229 oxidation HULIS also increase in water-insoluble chromophores (average 17.5%). Low-oxidation
 230 HULIS also decrease in water-insoluble chromophores. In ambient PM, the content of high-
 231 oxidation HULIS increase and the low-oxidation HULIS decrease (**Fig.4C**), which reveal that low-
 232 oxidation HULIS could be transformed into high-oxidation HULIS in aerosol aging process (Chen
 233 et al., 2016a). Thus, high-oxidation HULIS could be used to trace the aerosols aging degree.

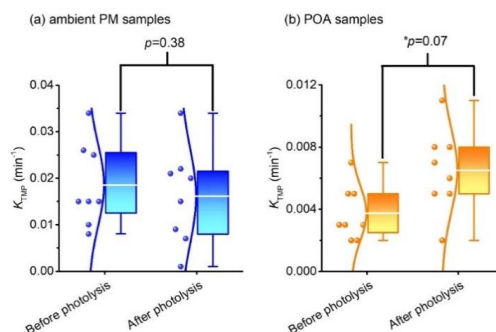


234
235
236
237

Fig.4 (A) The EEM spectra of chromophores; (B) is the variation characteristics of chromophores in POA; (C) is the variation characteristics of chromophores in ambient PM. *: The data of 3-day photolysis of water-soluble chromophores in winter is unavailable.

238 3.3 Effect of COM photo-degradation on aerosol photochemical reactivity

239 COM photo-degradation has a significant effect on aerosol photochemical reactivity. The
240 photochemical activity is characterized by triplet state and singlet oxygen. **Fig.5** show the difference
241 of triplet state generation capability before and after the photolysis (Details are shown in Figure S6
242 of SI). The generation rate of triplet state is decreased by 11% on average after COM photolysis in
243 ambient PM, while statistical analysis show that photo-degradation do not significant affect the
244 triplet state generation ($p = 0.38$, two-tailed test). On the contrary, the triplet states generation rate
245 markedly increases by 75% on average in POA ($p = 0.07$, two-tailed test), which indicate that COM
246 photo-degradation has a significant improvement effect on triplet state generation. COM are photo-
247 decomposed, while the triplet state generation ability remains unchanged or increase. The results
248 are not as expected. However, the result can be explained by recent study (Chen et al. 2020 for
249 ACPD): only a small number of chromophores have the ability to generate triplet states in aerosols.
250 The decomposition of most chromophores do not represent the decomposition of these specific
251 types of chromophores. We use a high concentration of TMP, in this case, TMP mainly capture
252 short-lived triplet state (Rosado-Lausell et al., 2013). Thus, chromophores that can form a short-
253 lived triplet state may not be reduced or even generated during the photolysis process.



254
255 **Fig.5** The changes of the triplet state generation capacity in (a) the ambient PM and (b) POA samples before and
256 after photolysis. The line from bottom to top in the box plots are minimum, first quartile, the average value (white
257 lines), third quartile, and maximum, respectively. The p -value is the probability that two sets of data have the same
258 level (two-tailed test). * represents a significant difference at the 0.1 level.

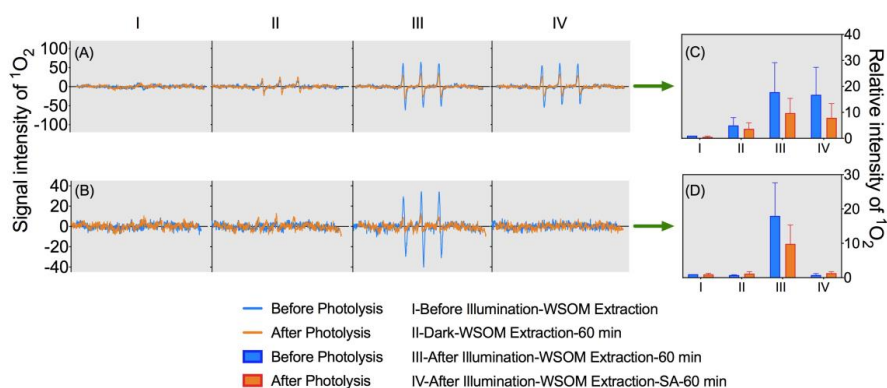
259 COM can generate triplet states and further induce singlet oxygen (McNeill and Canonica,
260 2016). The effects of COM photo-degradation on singlet oxygen are illustrated through the approach
261 of chemical capture and EPR analysis. Typical EPRs spectra of $^1\text{O}_2$ are shown in **Fig.6** (EPR spectra
262 of all samples are shown in Figure S7 and Figure S8). More narrowly, in the original POA samples
263 (i.e. the sample with photolysis time is 0, details of samples are described in section 2.2), there is
264 no significant $^1\text{O}_2$ signal before light excitation (the red curve in **Fig.6A (I)**) and only a small amount
265 of $^1\text{O}_2$ is generated after 60 min in dark (the red curve in **Fig.6A (II)**), which indicated that POA
266 has certain oxidability. As expected, compared with the sample without light excitation (the red
267 curve in **Fig. 6A (I)**), the signal intensity of $^1\text{O}_2$ increase by 3 times after 60 minutes of light
268 excitation (the red curve in **Fig. 6A (III)**), which prove the significant promoting effect of light on
269 $^1\text{O}_2$. However, $^1\text{O}_2$ is not reduced when the triplet state is quenched by sorbic acid (the red curve in
270 **Fig.6A (IV)**). Sorbic acid is a trapping agent of high-energy triplet state (triplet energies $E_T = 239$ -
271 247 kJ/mol) (Zhou et al., 2019; Moor et al., 2019), therefore, the above results indicate that the low-
272 energy $^3\text{COM}^*$ ($E_T < 239$ kJ/mol) may be the main precursor for $^1\text{O}_2$ ($E_T = 94$ kJ/mol) in POA.

273 The COM photo-degradation can change the yield of $^1\text{O}_2$. Compared with original POA
274 samples, the signal intensity of $^1\text{O}_2$ decrease significantly in the samples with 7 days of photolysis
275 (the blue curve in **Fig.6A**), with an average decrease of 42.1% (**Fig.6C**), which prove that photo-
276 degradation has a restraining effect on the photochemical activity in POA. Similar to the original
277 sample, the signal intensity of $^1\text{O}_2$ do not decrease obviously when the high-energy triplet states are
278 quenched by sorbic acid in the photolyzed samples. The mechanism is same as original samples.
279 The results also reveal that the COM photo-degradation process do not change the mechanism of
280 low-energy $^3\text{COM}^*$ inducing $^1\text{O}_2$ in POA.

281 The photochemical characteristics of ambient PM are different from POA. More narrowly,
282 there is no obvious $^1\text{O}_2$ signal in original ambient PM samples before light excitation (the red curve
283 in **Fig.6B (I)**). $^1\text{O}_2$ is also not generated after 60 min in dark (the red curve in **Fig.6B (II)**). The
284 content of $^1\text{O}_2$ increase significantly after 60 minutes of light excitation (the red curve in **Fig.6B**



285 (III)). When the triplet states are quenched by sorbic acid (Fig.6B(IV)), the signal of $^1\text{O}_2$ disappear.
286 The result suggests that $^1\text{O}_2$ is mainly induced by high-energy $^3\text{COM}^*$ in ambient PM. Compared
287 with the original samples, the signal intensity of $^1\text{O}_2$ decrease by 41.0% on average in photolyzed
288 samples (the red curve in Fig.6B). This characteristic reveal the restraining effect of COM photo-
289 degradation on photochemical activity in ambient PM. The restraining effect is similar to POA.
290 However, the quenching effect of sorbic acid on various aerosols are different (Fig.6 (IV)). The
291 above results directly prove that the precursor of high-energy triplet states could be photolyzed,
292 which directly lead to the decrease of $^1\text{O}_2$ yield in the ambient PM. Other experiments are needed
293 to prove whether the low-energy triplet precursors in POA are photolyzed and cause a decrease in
294 the yield of $^1\text{O}_2$.



295
296 **Fig.6** Variations of DOM inducing $^1\text{O}_2$ before and after photolysis. (A) and (C) are the results obtained from POA
297 samples. (B) and (D) are the results obtained from Ambient PM. The left of the figure was the EPR spectra of $^1\text{O}_2$.
298 The right of the figure was the content variations of $^1\text{O}_2$. Relative content was calculated with a standard of the signal
299 intensity of $^1\text{O}_2$. The standard is the signal intensity of $^1\text{O}_2$, which is induced by un-photolyzed and un-illuminated
300 samples.

301 4. Implication

302 The characteristics of COM photo-degradation and the effects of photo-degradation on the
303 photochemical activity in different aerosols are studied. Firstly, we prove that the photo-degradation
304 could lead to COM decompose and change in types. The conversion process of low-oxidation
305 HULIS to high-oxidation HULIS is observed in ambient PM, which reflect the significant influence
306 of photo-degradation on chemical composition. In turn, the attenuation and type conversion of COM
307 provide an important basis to trace the aerosol aging process. Optical properties are also effected by
308 COM photo-degradation. Secondly, we evaluate the effect of COM photo-degradation the
309 photochemical activity. Triplet state generation ability remain unchanged or increased in the aerosol
310 aging process, while photo-degradation has a significant restraining effect on the $^1\text{O}_2$ yield. So
311 photolysis and/or conversion of COM could be considered to be the main influence factor for
312 photochemical reaction capacity. In addition, the photochemical reaction mechanisms and aerosol
313 aging processes are relatively different in aerosols. It may be more useful to distinguish the types



314 of $^3\text{COM}^*$ into high and low energies, so that the mechanism of COM photochemical reaction can
315 be elucidated. In summary, the aerosol aging process has a remarkable impact on atmospheric
316 photochemistry. Aerosol aging can not only change the type and content of COM, but also change
317 their photochemical activity, which furtherly has a potential impact on the aerosol fate. Different
318 types of aerosols have different aging mechanisms, so the environmental impacts caused by COM
319 should also be different.

320 **Data availability.** All data that support the findings of this study are available in this article and its
321 Supplement or from the corresponding author on request.

322 **Supporting information.** Additional details, including Tables S1–S3, Figures S1–S8, calculation
323 of optical characteristics of WSOM/WISOM, are contained in the SI.

324 **Author contributions.** QC and ZM designed the experiments and data analysis. ZM and LZ
325 performed sample collection. ZM performed the photochemical experiment. ZM and DG performed
326 the OC/EC analysis and optical analysis. HL performed the EPR analysis. QC prepared the paper
327 with the contributions from all co-authors.

328 **Competing interests.** The authors declare that they have no conflict of interest.

329 **Acknowledgments.** We thank the National Natural Resources Foundation for its financial support.

330 **Financial support.** This work was supported by the National Natural Science Foundation of China
331 (grant numbers 41877354 and 41703102).

332 **References**

- 333 Aiona, P. K., Luek, J. L., Timko, S. A., Powers, L. C., Gonsior, M., and Nizkorodov, S. A.: Effect of Photolysis on
334 Absorption and Fluorescence Spectra of Light-Absorbing Secondary Organic Aerosols, *ACS Earth Space*
335 *Chem.*, 2, 235–245, 10.1021/acearthspacechem.7b00153, 2018.
- 336 Alfara, M. R., Prevot, A. S., Szidat, S., Sandradewi, J., Weimer, S., Lanz, V. A., Schreiber, D., Mohr, M., and
337 Baltensperger, U.: Identification of the mass spectral signature of organic aerosols from wood burning
338 emissions, *Environ. Sci. Technol.*, 41, 5770–5777, <http://dx.doi.org/10.1021/es062289b>, 2007.
- 339 Altieri, K. E., Carlton, A. G., Lim, H. J., Turpin, B. J., and Seitzinger, S. P.: Evidence for oligomer formation in
340 clouds: Reactions of isoprene oxidation products, *Environ. Sci. Technol.*, 40, 4956–4960,
341 <http://dx.doi.org/10.1021/es052170n>, 2006.
- 342 Altieri, K. E., Seitzinger, S. P., Carlton, A. G., Turpin, B. J., Klein, G. C., and Marshall, A. G.: Oligomers formed
343 through in-cloud methylglyoxal reactions: Chemical composition, properties, and mechanisms investigated by
344 ultra-high resolution FT-ICR mass spectrometry, *Atmos. Environ.*, 42, 1476–1490,
345 <http://dx.doi.org/10.1016/j.atmosenv.2007.11.015>, 2008.
- 346 Andreae, M. O., and Gelencser, A.: Black carbon or brown carbon? The nature of light-absorbing carbonaceous
347 aerosols, *Atmos. Chem. Phys.*, 6, 3131–3148, <http://dx.doi.org/10.5194/acp-6-3131-2006>, 2006.
- 348 Birdwell, J. E., and Engel, A. S.: Characterization of dissolved organicmatter in cave and spring waters using
349 UV–Vis absorbance andfluorescence spectroscopy, *Org. Geochem.*, 41,
350 <http://dx.doi.org/10.1016/j.orggeochem.2009.11.002>, 2010.
- 351 Chen, Q., Miyazaki, Y., Kawamura, K., Matsumoto, K., Coburn, S., Volkamer, R., Iwamoto, Y., Kagami, S., Deng,
352 Y., Ogawa, S., Ramasamy, S., Kato, S., Ida, A., Kajii, Y., and Mochida, M.: Characterization of Chromophoric
353 Water-Soluble Organic Matter in Urban, Forest, and Marine Aerosols by HR-ToF-AMS Analysis and



- 354 Excitation-Emission Matrix Spectroscopy, *Environ. Sci. Technol.*, 50, 10351-10360,
355 <http://dx.doi.org/10.1021/acs.est.6b01643>, 2016a.
- 356 Chen, Q., Mu, Z., Xu, L., Wang, M., Wang, J., Shan, M., Yang, X., Fan, X., Song, J., Wang, Y., Lin, P., Zhang, L.,
357 Shen, Z., and Du, L.: Triplet State Formation of Chromophoric Dissolved Organic Matter in Atmospheric
358 Aerosols: Characteristics and Implications, *Atmos. Chem. Phys. Discuss.*, [https://doi.org/10.5194/acp-2019-](https://doi.org/10.5194/acp-2019-1032)
359 1032, 2020.
- 360 Chen, Q., Li, J., Hua, X., Jiang, X., Mu, Z., Wang, M., Wang, J., Shan, M., Yang, X., Fan, X., Song, J., Wang, Y.,
361 Guan, D., and Du, L.: Identification of species and sources of atmospheric chromophores by fluorescence
362 excitation-emission matrix with parallel factor analysis, *Sci. Total Environ.*, 718, 137322,
363 <http://dx.doi.org/10.1016/j.scitotenv.2020.137322>, 2020.
- 364 Chen, Q. C., Ikemori, F., and Mochida, M.: Light Absorption and Excitation-Emission Fluorescence of Urban
365 Organic Aerosol Components and Their Relationship to Chemical Structure, *Environ. Sci. Technol.*, 50, 10859-
366 10868, <http://dx.doi.org/10.1021/acs.est.6b02541>, 2016b.
- 367 Chen, Y., Zhang, X., and Feng, S.: Contribution of the Excited Triplet State of Humic Acid and Superoxide Radical
368 Anion to Generation and Elimination of Phenoxyl Radical, *Environ. Sci. Technol.*, 52, 8283-8291,
369 <http://dx.doi.org/10.1021/acs.est.8b00890>, 2018.
- 370 Cheng, Y., He, K. B., Du, Z. Y., Engling, G., Liu, J. M., Ma, Y. L., Zheng, M., and Weber, R. J.: The characteristics
371 of brown carbon aerosol during winter in Beijing, *Atmos. Environ.*, 127, 355-364,
372 <http://dx.doi.org/10.1016/j.atmosenv.2015.12.035>, 2016.
- 373 Chin, Y. P., Aiken, G., and O'Loughlin, E.: Molecular weight, polydispersity, and spectroscopic properties of aquatic
374 humic substances, *Environ. Sci. Technol.*, 28, 1853-1858, <http://dx.doi.org/10.1021/es00060a015>, 1994.
- 375 Chow, J. C., Watson, J. G., Chen, L. W., Arnott, W. P., Moosmuller, H., and Fung, K.: Equivalence of elemental
376 carbon by thermal/optical reflectance and transmittance with different temperature protocols, *Environ. Sci.*
377 *Technol.*, 38, 4414-4422, <http://dx.doi.org/10.1021/es034936u>, 2004.
- 378 Chu, C. H., Lundeen, R. A., Sander, M., and McNeill, K.: Assessing the Indirect Photochemical Transformation of
379 Dissolved Combined Amino Acids through the Use of Systematically Designed Histidine-Containing
380 Oligopeptides, *Environ. Sci. Technol.*, 49, 12798-12807, <http://dx.doi.org/10.1021/acs.est.5b03498>, 2015.
- 381 Coble, P. G.: Marine optical biogeochemistry: the chemistry of ocean color, *Chem. Rev.*, 107, 402-418,
382 <http://dx.doi.org/10.1021/cr050350+>, 2007.
- 383 Cory, R. M., and McKnight, D. M.: Fluorescence spectroscopy reveals ubiquitous presence of oxidized and reduced
384 quinones in dissolved organic matter, *Environ. Sci. Technol.*, 39, 8142-8149,
385 <http://dx.doi.org/10.1021/es0506962>, 2005.
- 386 Del Vecchio, R., and Blough, N. V.: Photobleaching of chromophoric dissolved organic matter in natural waters:
387 kinetics and modeling, *Mar. Chem.*, 78, 231-253, [http://dx.doi.org/10.1016/S0304-4203\(02\)00036-1](http://dx.doi.org/10.1016/S0304-4203(02)00036-1), 2002.
- 388 Del Vecchio, R., and Blough, N. V.: On the origin of the optical properties of humic substances, *Environ. Sci.*
389 *Technol.*, 38, 3885-3891, <http://dx.doi.org/10.1021/es049912h>, 2004.
- 390 Duarte, R. M. B. O., Pio, C. A., and Duarte, A. C.: Spectroscopic study of the water-soluble organic matter isolated
391 from atmospheric aerosols collected under different atmospheric conditions, *Anal. Chim. Acta*, 530, 7-14,
392 <http://dx.doi.org/10.1016/j.aca.2004.08.049>, 2005.
- 393 Fellman, J. B., Miller, M. P., Cory, R. M., D'Amore, D. V., and White, D.: Characterizing Dissolved Organic Matter
394 Using PARAFAC Modeling of Fluorescence Spectroscopy: A Comparison of Two Models, *Environ. Sci.*
395 *Technol.*, 43, 6228-6234, <http://dx.doi.org/10.1021/es900143g>, 2009.
- 396 Gonsior, M., Peake, B. M., Cooper, W. T., Podgorski, D., D'Andrilli, J., and Cooper, W. J.: Photochemically induced
397 changes in dissolved organic matter identified by ultrahigh resolution fourier transform ion cyclotron resonance
398 mass spectrometry, *Environ. Sci. Technol.*, 43, 698-703, <http://dx.doi.org/10.1021/es8022804>, 2009.
- 399 Graber, E. R., and Rudich, Y.: Atmospheric HULIS: how humic-like are they? A comprehensive and critical review,
400 *Atmos. Chem. Phys.*, 6, 729-753, <http://dx.doi.org/10.5194/acp-6-729-2006>, 2006.
- 401 Grieshop, A. P., Donahue, N. M., and Robinson, A. L.: Laboratory investigation of photochemical oxidation of
402 organic aerosol from wood fires 2: analysis of aerosol mass spectrometer data, *Atmos. Chem. Phys.*, 9, 2227-
403 2240, <http://dx.doi.org/DOI.10.5194/acp-9-2227-2009>, 2009.
- 404 Haag, W. R., and Gassman, E.: Singlet oxygen in surface waters-Part II: Quantum yields of its production by some
405 natural humic materials as a function of wavelength, *Chemosphere*, 13, 641-650,
406 [http://dx.doi.org/10.1016/0045-6535\(84\)90200-5](http://dx.doi.org/10.1016/0045-6535(84)90200-5), 1984.
- 407 Haynes, J. P., Miller, K. E., and Majestic, B. J.: Investigation into Photoinduced Auto-Oxidation of Polycyclic
408 Aromatic Hydrocarbons Resulting in Brown Carbon Production, *Environ. Sci. Technol.*, 53, 682-691,
409 <http://dx.doi.org/10.1021/acs.est.8b05704>, 2019.
- 410 Holmes, B. J., and Petrucci, G. A.: Water-soluble oligomer formation from acid-catalyzed reactions of levoglucosan
411 in proxies of atmospheric aqueous aerosols, *Environ. Sci. Technol.*, 40, 4983-4989,
412 <http://dx.doi.org/10.1021/es060646c>, 2006.
- 413 Huguet, A., Vacher, L., Relexans, S., Saubusse, S., Froidefond, J. M., and Parlanti, E.: Properties of fluorescent
414 dissolved organic matter in the Gironde Estuary, *Org. Geochem.*, 40,
415 <http://dx.doi.org/10.1016/j.orggeochem.2009.03.002>, 2009.
- 416 Karanasiou, A., Mingüillón, M. C., Viana, M., Alastuey, A., Putaud, J.-P., Maenhaut, W., Panteliadis, P., Močnik,
417 G., Favez, O., and Kuhlbusch, T. A. J.: Thermal-optical analysis for the measurement of elemental carbon (EC)
418 and organic carbon (OC) in ambient air a literature review, *Atmos. Meas. Tech. Discuss.*, 8, 9649-9712,
419 <http://dx.doi.org/10.5194/amtd-8-9649-2015>, 2015.



- 420 Kaur, R., and Anastasio, C.: First Measurements of Organic Triplet Excited States in Atmospheric Waters, *Environ.*
421 *Sci. Technol.*, 52, 5218-5226, <http://dx.doi.org/10.1021/acs.est.7b06699>, 2018.
- 422 Kieber, R. J., Adams, M. B., Wiley, J. D., Whitehead, R. F., Avery, G. B., Mullaugh, K. M., and Mead, R. N.: Short
423 term temporal variability in the photochemically mediated alteration of chromophoric dissolved organic matter
424 (CDOM) in rainwater, *Atmos. Environ.*, 50, 112-119, <http://dx.doi.org/10.1016/j.atmosenv.2011.12.054>, 2012.
- 425 Korak, J. A., Dotson, A. D., Summers, R. S., and Rosario-Ortiz, F. L.: Critical analysis of commonly used
426 fluorescence metrics to characterize dissolved organic matter, *Water Res.*, 49, 327-338,
427 <http://dx.doi.org/10.1016/j.watres.2013.11.025>, 2014.
- 428 Latch, D. E., and McNeill, K.: Microheterogeneity of singlet oxygen distributions in irradiated humic acid solutions,
429 *Science*, 311, 1743-1747, <http://dx.doi.org/10.1126/science.1121636>, 2006.
- 430 Lee, H. J., Laskin, A., Laskin, J., and Nizkorodov, S. A.: Excitation-emission spectra and fluorescence quantum
431 yields for fresh and aged biogenic secondary organic aerosols, *Environ. Sci. Technol.*, 47, 5763-5770,
432 <http://dx.doi.org/10.1021/es400644c>, 2013.
- 433 Lee, H. J., Aiona, P. K., Laskin, A., Laskin, J., and Nizkorodov, S. A.: Effect of solar radiation on the optical
434 properties and molecular composition of laboratory proxies of atmospheric brown carbon, *Environ. Sci.*
435 *Technol.*, 48, 10217-10226, <http://dx.doi.org/10.1021/es502515r>, 2014.
- 436 Liu, J. M., Lin, P., Laskin, A., Laskin, J., Kathmann, S. M., Wise, M., Caylor, R., Imholt, F., Selimovic, V., and
437 Shilling, J. E.: Optical properties and aging of light-absorbing secondary organic aerosol, *Atmos. Chem. Phys.*,
438 16, 12815-12827, <http://dx.doi.org/10.5194/acp-16-12815-2016>, 2016.
- 439 Ma, J., Del Vecchio, R., Golanoski, K. S., Boyle, E. S., and Blough, N. V.: Optical properties of humic substances
440 and CDOM: effects of borohydride reduction, *Environ. Sci. Technol.*, 44, 5395-5402,
441 <http://dx.doi.org/10.1021/es100880q>, 2010.
- 442 Maizel, A. C., Li, J., and Remucal, C. K.: Relationships Between Dissolved Organic Matter Composition and
443 Photochemistry in Lakes of Diverse Trophic Status, *Environ. Sci. Technol.*, 51, 9624-9632,
444 <http://dx.doi.org/10.1021/acs.est.7b01270>, 2017.
- 445 Malley, P. P. A., Grossman, J. N., and Kahan, T. F.: Effects of Chromophoric Dissolved Organic Matter on
446 Anthracene Photolysis Kinetics in Aqueous Solution and Ice, *J. Phys. Chem. A*, 121, 7619-7626,
447 <http://dx.doi.org/10.1021/acs.jpca.7b05199>, 2017.
- 448 McKnight, D. M., Boyer, E. W., Westerhoff, P. K., Doran, P. T., Kulbe, T., and Andersen, D. T.: Spectrofluorometric
449 characterization of dissolved organic matter for indication of precursor organic material and aromaticity,
450 *Limnol. Oceanogr.*, 46, 38-48, <http://dx.doi.org/10.4319/lo.2001.46.1.0038>, 2001.
- 451 McNeill, K., and Canonica, S.: Triplet state dissolved organic matter in aquatic photochemistry: reaction
452 mechanisms, substrate scope, and photophysical properties, *Environ. Sci. Process Impacts*, 18, 1381-1399,
453 <http://dx.doi.org/10.1039/c6em00408c>, 2016.
- 454 Moor, K. J., Schmitt, M., Erickson, P. R., and McNeill, K.: Sorbic Acid as a Triplet Probe: Triplet Energy and
455 Reactivity with Triplet-State Dissolved Organic Matter via $^{1}O_2$ Phosphorescence, *Environ. Sci. Technol.*,
456 <http://dx.doi.org/10.1021/acs.est.9b01787>, 2019.
- 457 Mu, Z., Chen, Q. C., Wang, Y. Q., Shen, Z. X., Hua, X. Y., Zhang, Z. M., Sun, H. Y., Wang, M. M., and Zhang, L.
458 X.: Characteristics of Carbonaceous Aerosol Pollution in PM_{2.5} in Xi'an, *Huan Jing Ke Xue*, 40, 1529-1536,
459 <http://dx.doi.org/10.13227/j.hj.kx.201807135>, 2019.
- 460 Murphy, K. R., Stedmon, C. A., Waite, T. D., and Ruiz, G. M.: Distinguishing between terrestrial and autochthonous
461 organic matter sources in marine environments using fluorescence spectroscopy, *Mar. Chem.*, 108, 40-58,
462 <http://dx.doi.org/10.1016/j.marchem.2007.10.003>, 2008.
- 463 Murphy, K. R., Stedmon, C. A., Graeber, D., and Bro, R.: Fluorescence spectroscopy and multi-way techniques.
464 PARAFAC, *Anal. Methods*, 5, 6557-6566, <http://dx.doi.org/10.1039/c3ay41160e>, 2013.
- 465 Paul Hansard, S., Vermilyea, A. W., and Voelker, B. M.: Measurements of superoxide radical concentration and
466 decay kinetics in the Gulf of Alaska, *Deep Sea Res., Part I*, 57, 1111-1119,
467 <http://dx.doi.org/10.1016/j.dsr.2010.05.007>, 2010.
- 468 Perri, M. J., Seitzinger, S., and Turpin, B. J.: Secondary organic aerosol production from aqueous photooxidation of
469 glycolaldehyde: Laboratory experiments, *Atmos. Environ.*, 43, 1487-1497,
470 <http://dx.doi.org/10.1016/j.atmosenv.2008.11.037>, 2009.
- 471 Powers, L. C., Babcock-Adams, L. C., Enright, J. K., and Miller, W. L.: Probing the photochemical reactivity of
472 deep ocean refractory carbon (DORC): Lessons from hydrogen peroxide and superoxide kinetics, *Mar. Chem.*,
473 177, 306-317, [10.1016/j.marchem.2015.06.005](https://doi.org/10.1016/j.marchem.2015.06.005), 2015.
- 474 Richards-Henderson, N. K., Pham, A. T., Kirk, B. B., and Anastasio, C.: Secondary organic aerosol from aqueous
475 reactions of green leaf volatiles with organic triplet excited states and singlet molecular oxygen, *Environ. Sci.*
476 *Technol.*, 49, 268-276, <http://dx.doi.org/10.1021/es503656m>, 2015.
- 477 Rosado-Lausell, S.L., Wang, H.T., Gutierrez, L., Romero-Maraccini, O.C., Niu, X.Z., Gin, K.Y.H., Croue, J.P.,
478 Nguyen, T.H.: Roles of singlet oxygen and triplet excited state of dissolved organic matter formed by different
479 organic matters in bacteriophage MS2 inactivation, *Water Res.*, 47, 4869-4879,
480 <http://dx.doi.org/10.1016/j.watres.2013.05.018>, 2013.
- 481 Rosario-Ortiz, F. L., and Canonica, S.: Probe Compounds to Assess the Photochemical Activity of Dissolved
482 Organic Matter, *Environ. Sci. Technol.*, 50, 12532-12547, <http://dx.doi.org/10.1021/acs.est.6b02776>, 2016.
- 483 Saleh, R., Hennigan, C. J., McMeeking, G. R., Chuang, W. K., Robinson, E. S., Coe, H., Donahue, N. M., and
484 Robinson, A. L.: Absorptivity of brown carbon in fresh and photo-chemically aged biomass-burning emissions,
485 *Atmos. Chem. Phys.*, 13, 7683-7693, <http://dx.doi.org/10.5194/acp-13-7683-2013>, 2013.



- 486 Sharpless, C. M.: Lifetimes of Triplet Dissolved Natural Organic Matter (DOM) and the Effect of NaBH₄ Reduction
487 on Singlet Oxygen Quantum Yields: Implications for DOM Photophysics, *Environ. Sci. Technol.*, 46, 4466-
488 4473, <http://dx.doi.org/10.1021/es300217h>, 2012.
- 489 Sierra, M. M. D., Giovanela, M., Parlanti, E., and Soriano-Sierra, E. J.: Fluorescence fingerprint of fulvic and humic
490 acids from varied origins as viewed by single-scan and excitation/emission matrix techniques, *Chemosphere*,
491 58, <http://dx.doi.org/10.1016/j.chemosphere.2004.09.038>, 2005.
- 492 Smith, J. D., Sio, V., Yu, L., Zhang, Q., and Anastasio, C.: Secondary organic aerosol production from aqueous
493 reactions of atmospheric phenols with an organic triplet excited state, *Environ. Sci. Technol.*, 48, 1049-1057,
494 <http://dx.doi.org/10.1021/es4045715>, 2014.
- 495 Szymczak, R., and Waite, T.: Generation and decay of hydrogen peroxide in estuarine waters, *Mar. Freshwater Res.*,
496 39, 289-299, <http://dx.doi.org/10.1071/MF9880289>, 1988.
- 497 Tang, S. S., Li, F. H., Tsona, N. T., Lu, C. Y., Wang, X. F., and Du, L.: Aqueous-Phase Photooxidation of Vanillic
498 Acid: A Potential Source of Humic-Like Substances (HULIS), *ACS Earth and Space Chem.*, 4, 862-872,
499 <http://dx.doi.org/10.1021/acsearthspacechem.0c00070>, 2020.
- 500 Vodacek, A., Blough, N. V., DeGrandpre, M. D., Peltzer, E. T., and Nelson, R. K.: Seasonal Variation of
501 CDOM and DOC in the Middle Atlantic Bight: Terrestrial Inputs and Photooxidation, *Limnol.*
502 *Oceanogr.*, 42, 231-253, <http://dx.doi.org/10.1117/12.26643>, 1997.
- 503 Wenk, J., von Gunten, U., and Canonica, S.: Effect of dissolved organic matter on the transformation of contaminants
504 induced by excited triplet states and the hydroxyl radical, *Environ. Sci. Technol.*, 45, 1334-1340,
505 <http://dx.doi.org/10.1021/es102212t>, 2011.
- 506 Wenk, J., Aeschbacher, M., Salhi, E., Canonica, S., von Gunten, U., and Sander, M.: Chemical oxidation of dissolved
507 organic matter by chlorine dioxide, chlorine, and ozone: effects on its optical and antioxidant properties,
508 *Environ. Sci. Technol.*, 47, 11147-11156, <http://dx.doi.org/10.1021/es402516b>, 2013.
- 509 Wong, J. P. S., Zhou, S. M., and Abbatt, J. P. D.: Changes in Secondary Organic Aerosol Composition and Mass
510 due to Photolysis: Relative Humidity Dependence, *J. Phys. Chem. A*, 119, 4309-4316,
511 <http://dx.doi.org/10.1021/jp506898c>, 2015.
- 512 Zappoli, S., Andracchio, A., Fuzzi, S., Facchini, M. C., Gelencser, A., Kiss, G., Krivacsy, Z., Molnar, A., Meszaros,
513 E., Hansson, H. C., Rosman, K., and Zebuhr, Y.: Inorganic, organic and macromolecular components of fine
514 aerosol in different areas of Europe in relation to their water solubility, *Atmos. Environ.*, 33, 2733-2743,
515 [http://dx.doi.org/10.1016/S1352-2310\(98\)00362-8](http://dx.doi.org/10.1016/S1352-2310(98)00362-8), 1999.
- 516 Zepp, R. G., Schlotzhauer, P. F., and Sink, R. M.: Photosensitized transformations involving electronic energy
517 transfer in natural waters: role of humic substances, *Environ. Sci. Technol.*, 19, 74-81,
518 <http://dx.doi.org/10.1021/es00131a008>, 1985.
- 519 Zhang, D., Yan, S., and Song, W.: Photochemically induced formation of reactive oxygen species (ROS) from
520 effluent organic matter, *Environ. Sci. Technol.*, 48, 12645-12653, <http://dx.doi.org/10.1021/es5028663>, 2014.
- 521 Zhao, R., Lee, A. K. Y., Huang, L., Li, X., Yang, F., and Abbatt, J. P. D.: Photochemical processing of aqueous
522 atmospheric brown carbon, *Atmos. Chem. Phys.*, 15, 6087-6100, <http://dx.doi.org/10.5194/acp-15-6087-2015>,
523 2015.
- 524 Zhong, M., and Jang, M.: Dynamic light absorption of biomass-burning organic carbon photochemically aged under
525 natural sunlight, *Atmos. Chem. Phys.*, 14, 1517-1525, <http://dx.doi.org/10.5194/acp-14-1517-2014>, 2014.
- 526 Zhou, H., Yan, S., Lian, L., and Song, W.: Triplet-State Photochemistry of Dissolved Organic Matter: Triplet-State
527 Energy Distribution and Surface Electric Charge Conditions, *Environ. Sci. Technol.*, 53, 2482-2490,
528 <http://dx.doi.org/10.1021/acs.est.8b06574>, 2019.